ELSEVIER

PII: S0032-3861(97)10349-4

Polymer Vol. 39 No. 17, pp. 3945–3953, 1998

0032-3861/98/$19.00+0.00

Tensile drawing of ethylene/vinyl-alcohol copolymers. Part 1. Influence of draw temperature on the mechanical behaviour

Karina Djezzar[a], Laurence Penel[a], Jean-Marc Lefebvre[a], Roland Séguéla[a,*] and Yves Germain[b]

[a]*Laboratoire 'Structure et Propriétés de l'Etat Solide', URA CNRS 234, Université des Sciences et Technologies de Lille, Bât. C6, 59655 Villeneuve d'Ascq Cédex, France*
[b]*Centre d'Etudes 'Recherche et Développement', ELF-ATOCHEM, 27470 Serquigny, France*
(Received 14 February 1997; revised 23 June 1997; accepted 25 November 1997)

The uniaxial tensile drawing of two vinyl-alcohol-rich ethylene/vinyl-alcohol copolymers differing in composition and melt flow index is studied as a function of draw temperature. A change of mechanical properties occurs in the strain range of the strain-hardening threshold depending on whether the draw temperature is above or below a critical value of about 100°C. A strong propensity for necking and concomitant longitudinal fissuration of the films take place above this temperature for the copolymer of lower vinyl-alcohol content. The vinyl-alcohol richer copolymer, having a higher melting point and a lower melt flow index, exhibits similar trends at higher temperatures. Bulk materials also display longitudinal fissures originating from transverse craze-like defects located along the neck shoulder. It is suggested that the drastic weakening of the van der Waals (v.d.w.) interactions of paraffinic nature between the hydrogen-bonded sheets of the monoclinic crystal structure, above 100°C, results in a strong mechanical anisotropy. This may perfectly account for the fissuring trend thanks to the easy glide of the weakly interacting sheets. In contrast, a strain-induced disorganization of the crystalline structure triggers improved drawability to the copolymers at low draw temperature, owing to the mechanical isotropy of the new mesomorphic structure type.

(Keywords: ethylene/vinyl-alcohol copolymers; tensile drawing; yield behaviour)

INTRODUCTION

Poly(vinyl alcohol) (PVOH) and vinyl-alcohol-rich copolymers with ethylene (EVOH) are highly efficient gas barrier materials[1,2]. They have great potential for food packaging applications, but they need to be associated with polyolefins into multilayer films in order to prevent water absorption that reduces the gas barrier properties[3]. Unlike polypropylene (PP) and polyethylene (PE), however, which can be easily biaxially oriented at temperatures close to the melting point[4–9], these materials display very poor capability for biaxial drawing because of a high propensity for fibrillation. However, it has been reported that 3 × 3 biaxial drawing of EVOH copolymers can be performed simultaneously at low draw temperatures[3], namely in the range 80–100°C, and even sequentially in the temperature range 50–80°C. Such biaxially oriented sheets exhibit improved mechanical strength and better gas barrier properties compared with unoriented films[3].

Similar problems towards biaxial orientation have also been reported for polyamides, which require low temperature biaxial drawing[3]. It seems that the strong chain interactions, due to hydrogen bonding, are the main cause of the rather odd drawing behaviour of these materials. In this connection, it has been stated that strong cohesive energy polymers exhibit high rates of orientation-induced crystallization during the first drawing stage, which is prejudicial to the second stage[10].

The understanding of the problems encountered during biaxial orientation involves a better knowledge of the uniaxial orientation mechanisms. Much work has been done regarding the mechanical and structural aspects of the plastic deformation of polyamides (see Refs 11–13 and the references cited therein), but PVOH and related EVOH copolymers have, as yet, received little attention. This paper deals with the influence of temperature on the tensile drawing behaviour of vinyl-alcohol-rich EVOH copolymers from the standpoints of both mechanical properties and macroscopic structural characteristics upon deformation. Preliminary work has already been published elsewhere[14].

EXPERIMENTAL

Two ethylene/vinyl-alcohol copolymers from Nippon Gohsei have been investigated. Their characteristics are reported in *Table 1*. The materials were melt-cast into films about 200 μm thick from a T-die extruder at 210°C and cooled on a chill roll at a temperature of 90°C. Owing to imperfect extrusion conditions, these films had a wavy surface and, consequently, an uneven thickness with 10% local variations about the average value.

Sheets about 2 mm thick were also prepared by compression moulding stacks of 12 film plies at 210°C, between Teflon-coated steel plates. Each film pile was

* To whom correspondence should be addressed

previously dried by gradual heating to 210°C in a vacuum oven in order to eliminate the absorbed water and avoid any bubble formation due to vaporization from the molten polymer. It was then transferred into the compression-moulding press and finally cooled down to room temperature at about 20°C min^{-1}. Both films and bulk plates were stored until drawing at room temperature and about 50% R.H. Some of the samples have been studied in a 'dried state' after storage for 2 weeks in the presence of freshly regenerated molecular sieves, at room temperature. Moisture-saturated samples were prepared by immersing into water for 2 weeks, at room temperature.

The drawing experiments were conducted at a cross-head speed of 50 mm min^{-1} in an Instron tensile testing machine equipped with an air-pulsed oven regulated at ±1°C. Local draw ratios, $\lambda = l/l_0$, were directly measured on the samples from the spacing of ink marks printed 1.5 mm apart prior to drawing. Macroscopic draw ratios, $\Lambda = L/L_0$, are defined from the change of the sample gauge length. Different kinds of experiment were performed as follows:

(1) dumbbell-shaped samples with gauge dimensions 24 mm in length and 5 mm in width were cut out from the films and drawn as a function of temperature. The curves reported are the ones closer the average of four measurements at every temperature;
(2) samples of the same type as above were cut off the thick plates and drawn at 80 and 120°C, to perform X-ray diffraction experiments and morphological observations;
(3) film strips 60 mm long and 35 mm wide were used for two-step drawing experiments. In the first step, the strips were drawn at various temperatures in the range 70–140°C, up to a constant draw ratio $\lambda \approx 4$. Then, dumbbell-shaped specimens were cut out in the longitudinal direction of these drawn strips and redrawn at 70°C. The yield stress data reported are average values of four measurements;
(4) film specimens, 10 mm in gauge length and 70 mm in width, were drawn in close-to plane strain conditions, for morphological characterization. This experiment simulates the first-step of sequential biaxial orientation, i.e. uniaxial drawing at constant width.

The viscoelastic behaviour was analysed in tensile mode on a Rheometrics RSA II equipment at a frequency of 1 Hz. The test pieces were rectangular strips 20–25 mm long and 6 mm wide.

Differential scanning calorimetry (d.s.c.) was carried out using Perkin–Elmer DCS-7-Delta apparatus. The heating and cooling rates were 10°C min^{-1} and the sample weight was about 5 mg. Calibration of temperature and heat flow at the same scanning rate was achieved with high purity indium and zinc reference samples. The weight fraction crystallinity X_c of the samples was calculated from the ratio of the enthalpy of fusion of the sample ΔH_f to that of an infinitely large perfect crystal of the copolymer ΔH_f°. The assumed value $\Delta H_f^\circ = 117 \pm 3$ J g^{-1} is an average value taken from literature data[3,15] regarding three copolymers having ethylene concentrations in the range 30–44 mol%.

Wide-angle X-ray scattering (WAXS) patterns were recorded on flat films using the nickel-filtered Cu Kα radiation from a Philips tube operated at 40 kV and 20 mA.

Low magnification photographs of the drawn films were taken with a Konica camera, by placing the samples between crossed polarizers, in transmitted light. Optical micrographs from films as well as bulk samples were recorded on an Olympus BH-2 polarizing microscope provided with a polychromatic light source.

Table 1 Characteristics of the polymers as supplied

Material	EMF[a]	MFI[b] (g 10 min^{-1})	Density (g cm^{-3})	T_g (°C)	T_c (°C)	T_f (°C)	X_c [c]
Soarnol A	0.44	12	1.14	37	143	162	0.60
Soarnol DC	0.32	3.2	1.19	41	160	180	0.70

[a] EMF = ethylene molar fraction
[b] MFI = melt flow index
[c] crystal weight fraction measured on dried samples

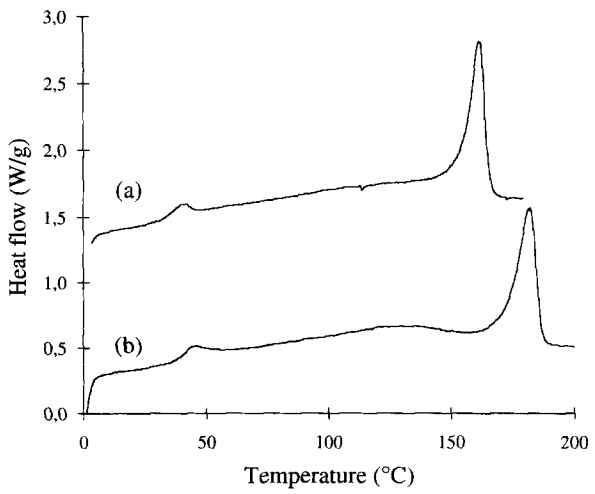

Figure 1 D.s.c. heating curves of the cast films of (*a*) copolymer A and (*b*) copolymer DC at an initial relative humidity of 50%

RESULTS AND DISCUSSION

Thermal behaviour

The d.s.c. curves of the raw copolymer films, for a room temperature relative humidity of about 50%, are shown in *Figure 1*. A clear-cut heat capacity jump related to the glass transition appears for both copolymers A and DC. This is rather unusual for semi-crystalline polymers having a crystal weight fraction beyond 70% (*Table 1*).

The degree of relative humidity significantly alters the glass transition temperature. For instance, moisture-saturated samples have a glass transition temperature T_g about 10°C below that of the corresponding sample of *Figure 1*. Conversely, samples in equilibrium with a dried atmosphere have a T_g about 10°C above. The melting point is little affected by the relative humidity, indicating that water is mainly sorbed in the amorphous phase. The characteristic thermal parameters of the dried samples are reported in *Table 1*.

Worth mentioning is the broad endotherm spanning the temperature range between the glass transition and the melting peak that results from the release of the sorbed water. This phenomenon partially blurs the onset of the melting peak; therefore, the use of d.s.c. to probe the structural changes induced by drawing requires that the samples are dried prior to the heating scan. In addition, this should be achieved at room temperature in order to avoid any post-drawing annealing effect. However, the fact that the T_g of a sample dried at room temperature is about 5°C higher for the second d.s.c. run compared with that after the

first run indicates that some water is expelled while heating beyond the melting point. This means that some complexed water molecules remain in the amorphous phase even after a drying treatment.

Dynamic mechanical behaviour

The dynamic mechanical spectra of *Figure 2* show that the two copolymers exhibit the three main relaxations characteristic of PVOH. The high temperature α relaxation, which accounts for the activation of molecular mobilities within the crystalline phase[16] or close to the crystal lamellae surface[17], occurs at 110°C and 120°C for copolymers A and DC respectively. This difference accounts for the higher melting point of copolymer DC. The α relaxation is roughly insensitive to the moisture content. In consideration of the melting behaviour discussed above, this finding supports the assignment of this relaxation to the purely crystalline part of the material.

The intermediate β relaxation, that is unanimously associated with the cooperative motions of hydrogen-bonded amorphous chains[16,18,19], is strongly affected by the sorbed water. Both temperature and magnitude of the β peak are modified. Increasing moisture content decreases the β peak temperature, indicating improved chain mobility in the amorphous phase. This feature is qualitatively consistent with the d.s.c. analysis of the glass transition. The magnitude of the β relaxation increases significantly for the moisture-saturated sample as it merges into the lower γ relaxation. As a matter of fact, the latter relaxation is associated with non-bonded amorphous chains[16], so that when all the intermolecular H-bonds are broken by water molecules, the two relaxations become indiscernible and gather into a single peak.

Tensile drawing behaviour

The nominal stress–strain curves of copolymers A and DC are shown in *Figure 3*. For both copolymers, a sharp yield point that is relevant to a necking phenomenon appears as the first step of the plastic deformation at 60°C, i.e. about the glass transition temperature. The draw plateau characteristic of a neck propagation is followed by a strong strain-hardening stage. Both the stress drop at yield and the strain-hardening rate are gradually reduced with increasing temperature. Considering that temperature has no major effect on structure and crystal content before 140°C and 160°C for copolymers A and DC respectively, the above changes may be ascribed to a crystalline phase softening due to the activation of the crystalline mechanical relaxation at

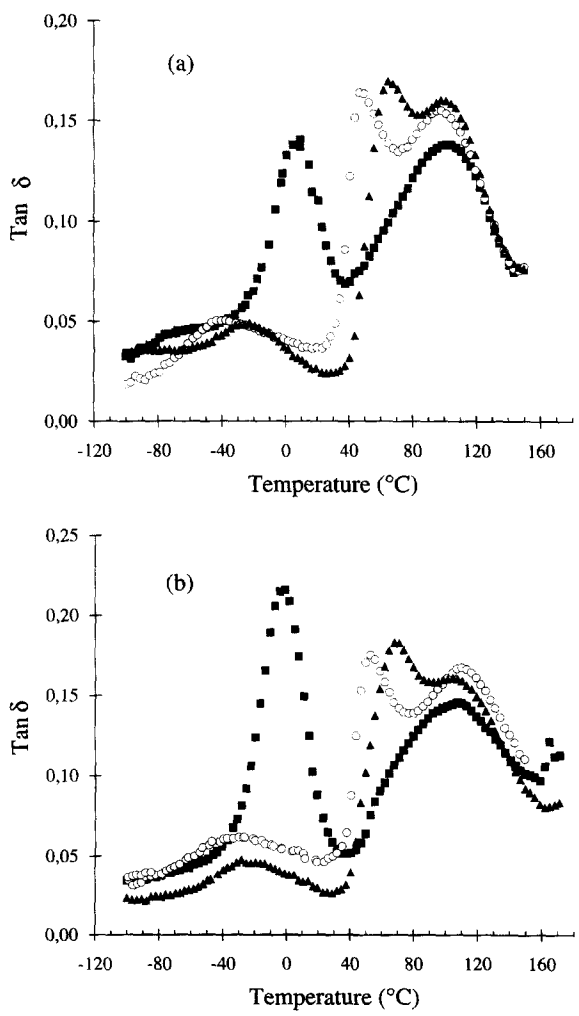

Figure 2 Loss factor tan δ *versus* temperature for (*a*) copolymer A and (*b*) copolymer DC: (▲) dried, (○) 50% R.H., (■) moisture-saturated

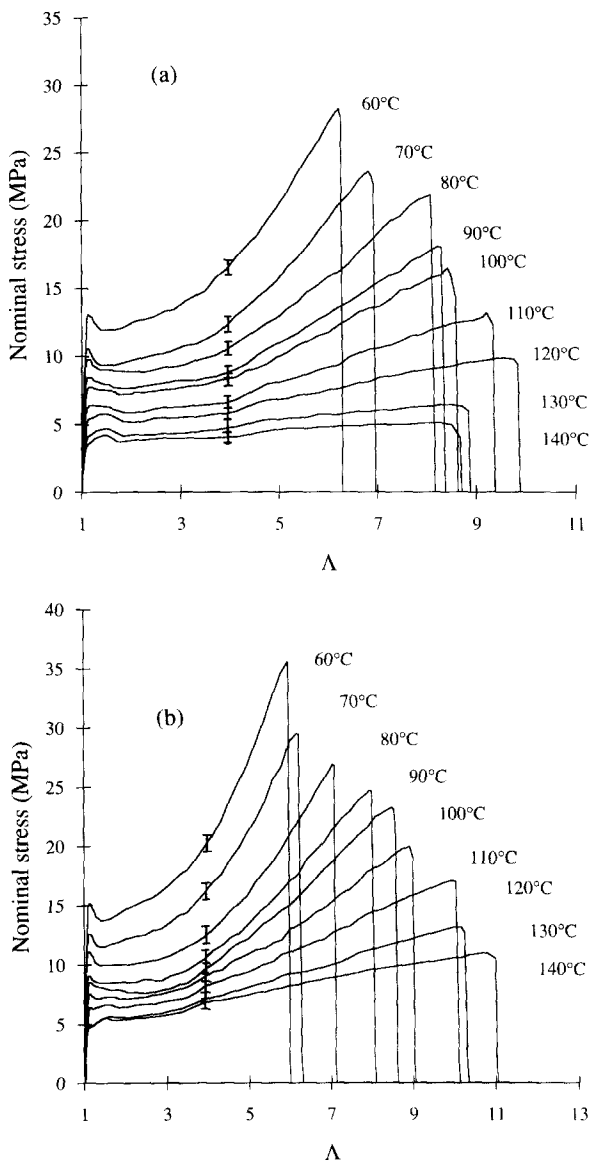

Figure 3 Nominal stress–strain curves of (*a*) copolymer A and (*b*) copolymer DC as a function of the draw temperature (the 'I' symbol is the average error bar of the stress measurement)

about $T \geq 40°C$ (see *Figure 2a* and *b*). It is noteworthy that, at equivalent temperature and the same draw ratio, both the draw stress and the strain-hardening are always greater for copolymer DC than copolymer A, although their crystallinities are very similar. This is certainly due to the higher molecular weight of the former material (see the melt flow index in *Table 1*) which brings about an additional effect of solid state viscosity.

The evolution of the nominal stress in the draw plateau, during the neck propagation, deserves some comment. At $T_d = 60°C$, i.e. in the temperature range of the glass transition as judged from the tan δ curve of *Figure 2*, drawing proceeds with an accompanying slight increase of the nominal stress up to $\lambda = 4$, where strain-hardening begins. This may be ascribed to non-linear viscoelastic effects in the amorphous phase having characteristic relaxation times in the range of the time scale of the experiment. Indeed, for strains beyond the yield point, the stress acting on the material out of the neck involves a structural evolution due to viscoelastic creep. This may be viewed as the preorientation of amorphous tie molecules prior to crystal chain unfolding. A slight strain-hardening results in these undrawn regions that makes neck propagation increasingly difficult as a function of time. In contrast, for $T_d = 20°C$, i.e. far below T_g (not shown in *Figure 2*), the nominal stress in the draw plateau is constant, indicating that propagation of the neck is a stationary process. In this case the relaxation times in the glassy amorphous phase are large compared with the duration of the drawing event so that any structural evolution in the undrawn regions is prohibited before plastic deformation proceeds via the neck shoulder advancement. A similar behaviour of constant nominal stress in the draw plateau is observed for $T_d > 80°C$, i.e. well above T_g. The relaxation times in the rubbery amorphous phase are then extremely short and no structural evolution is expected to occur in the undrawn parts which undergo purely elastic strains before the neck arrives.

The elongation at break increases with increasing temperature due to improved crystal ductility as the molecular mobilities of the α relaxation are activated. It drops as the draw temperature approaches the melting point. This is due to an early rupture of the material before the neck has propagated over the whole length of the sample owing to the very high ductility of the nearly molten crystals that readily creep under stress.

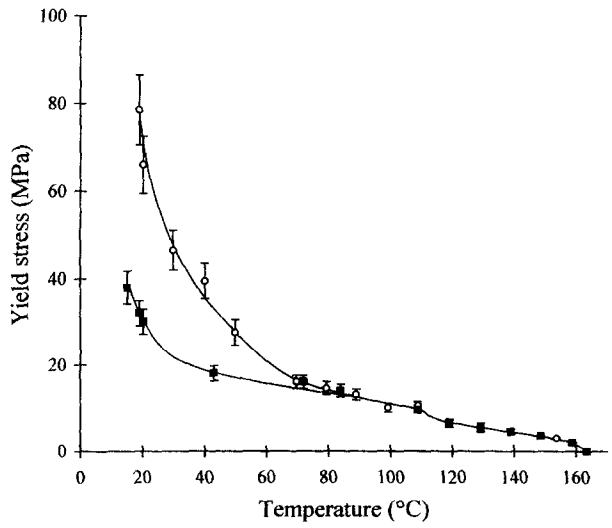

Figure 4 Yield stress variation with draw temperature of copolymer A: (○) 50% R.H. samples, (■) moisture-saturated prior to the measurement

Figure 4 shows that the yield stress of copolymer A drops steeply with increasing temperature below T_g, then decreases slowly from T_g up to the melting point. Taking into account the error bars on the stress data, a faint plateau can be seen at about 90–110°C, i.e. just below the α mechanical relaxation (see *Figure 2a*). In consideration that plasticity mainly relies on the phenomenon of crystal slip due to glide of dislocations along crystallographic planes, the applied stress should normally fall with increasing temperature thanks to the weakening of the molecular interactions. A speculative interpretation for the observed levelling of the yield stress is that an additional energy to the Peierls potential barrier for the dislocation glide arises from the activation of the rotational motions of the α relaxation. The consequence is that the mechanical energy absorption due to these motions momentarily hinders the glide process in the crystal.

The data from moisture-saturated samples just prior to the measurements (*Figure 4*) show that water-plasticization only occurs below T_g. This is additional evidence that water is only absorbed by the amorphous phase.

A quite unusual phenomenon has been reported in our previous work[14] in the case of copolymer A: in the temperature range 90–120°C, the strain-hardening region of the stress–strain curves displayed only very weak temperature dependence. It was suggested that two kinds of deformation regime prevail with respect to the draw temperature: namely a low temperature regime and a high temperature one. In the present series of experiments, this effect is much less obvious than previously reported for copolymer A (see the stress–strain curves at 90 and 100°C in *Figure 3a*), and for copolymer DC as well (*Figure 3b*). The most likely reason is that the films used in this study have a greater thickness irregularity than those of the previous work, so that the stress uncertainty does not allow one to detect the subtle changes in mechanical behaviour (see the error bars on the curves of *Figure 3*).

In order to investigate the changes of plastic behaviour that might eventually take place in the strain-hardening range (at about 100°C), a series of samples of each copolymer were drawn up to the same draw ratio $\lambda \approx 4$ at various temperatures in the range $70 < T < 140°C$. Then the samples were redrawn longitudinally at 70°C. The yield stress for redrawing is reported in *Figure 5* as a function of the temperature of the first step draw. Both copolymers exhibit a jump of the redrawing yield stress in the temperature range 80–100°C followed by a plateau. This suggests that two kinds of structure build up in the samples during the first step drawing, depending on whether the draw temperature is below or above the critical range, with the high temperature structure being stiffer than the low temperature one.

Morphological aspects of the plastic deformation

The EVOH copolymer displays, upon drawing in the high temperature range, very peculiar morphological characteristics that deserve special attention. *Figure 6* shows the necking features that occur during drawing of a thick sheet of copolymer A at 120°C. Before the yield point, sparse superficial cracks, a few hundred micrometres wide, develop transverse to the draw direction in the front view of the sample (*Figure 6a*). Surface defects are suspected to act as initiators for these cracks. Beyond the yield point, the cracks turn into roughly rectangular craze-like defects

(*Figure 6b*) in which the material seems pulled from the crack lips.

The drawing of thick sheets of copolymer A at 80°C involves homogeneous deformation devoid of cracks.

Thin films drawn in plane strain conditions, i.e. using samples much wider than long, behave somewhat differently. The photographs of *Figure 7* show that, at a draw temperature T_d = 80°C, copolymer A deforms nearly homogeneously. The rather broad interference fringes clearly denote the gradual thinning of the film from the regions close to the clamps towards the centre. Increasing the draw temperature to T_d = 120°C results in a more heterogeneous deformation, as indicated by the sharpening of the interference fringes. The central darker zone, which reveals the necked region, is related to both the low thickness and the strong chain orientation due to high strain. At $T_d > 120$°C, longitudinal fissures develop in the necked region. This is suggestive of a drop in the molecular cohesion, notably in the crystalline phase.

Copolymer DC displays similar morphological characteristics (*Figure 7e–h*). However, the temperature at which fissures occur is about 20°C higher than for copolymer A. This is certainly due to the higher melting point and higher molar weight (see the met flow indexes in *Table 1*) that both improve chain cohesion.

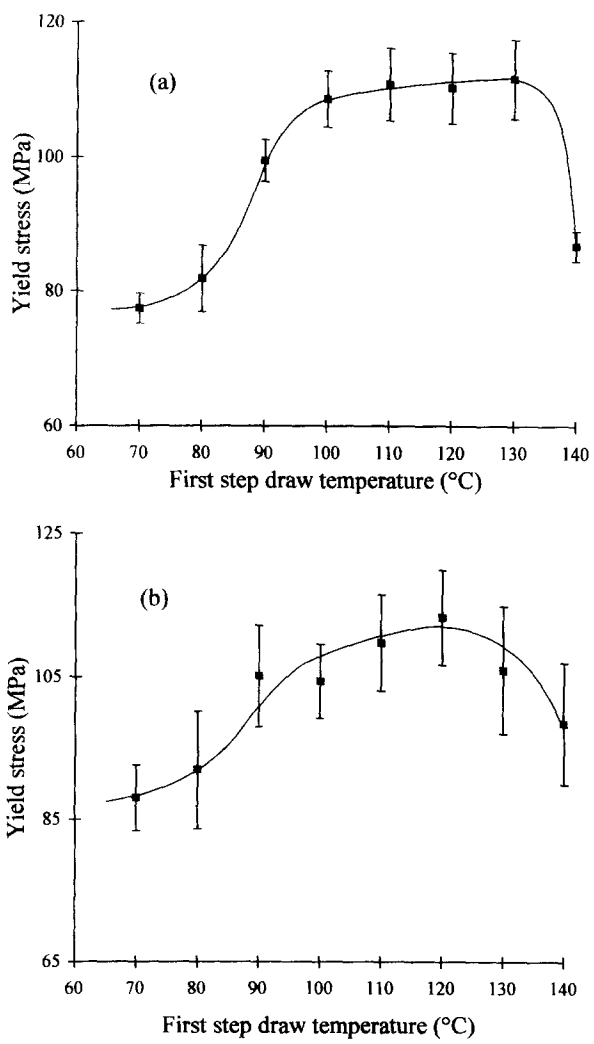

Figure 5 Yield stress for the longitudinal redrawing at 70°C of samples previously drawn up to $\lambda \approx 4$ as a function of the temperature of the first step drawing: (*a*) copolymer A and (*b*) copolymer DC

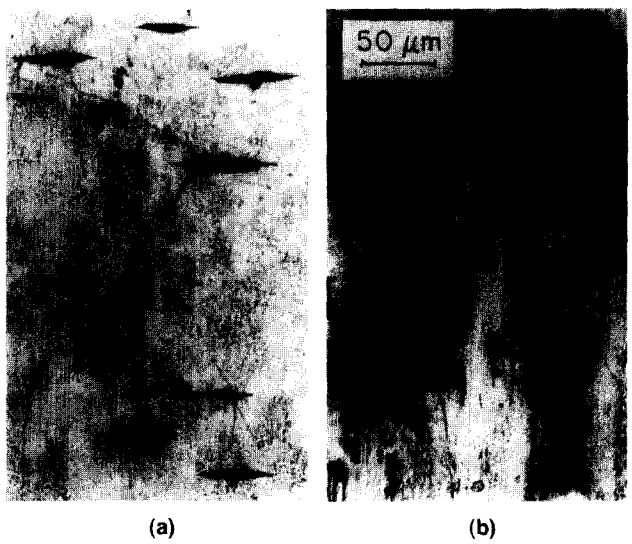

Figure 6 Optical micrographs of a thick sheet of copolymer A drawn at T_d = 120°C: face view (*a*) prior to the yield point and (*b*) beyond the yield point (crossed polarizers; draw axis vertical). Reproduced from Ref. [14] with permission of the American Society of Mechanical Engineers (ASME)

A close observation of the longitudinal fissures shows that they propagate from one neck shoulder towards the opposite one, as shown in *Figure 8a*. Indeed, these fissures are initiated from very small rectangular craze-like defects, such as that shown in *Figure 8b*, which develop in the neck shoulder probably due to the high strain gradient (the dark horizontal line is the contrasted neck shoulder). This kind of defect is very similar to those which occur in the front face

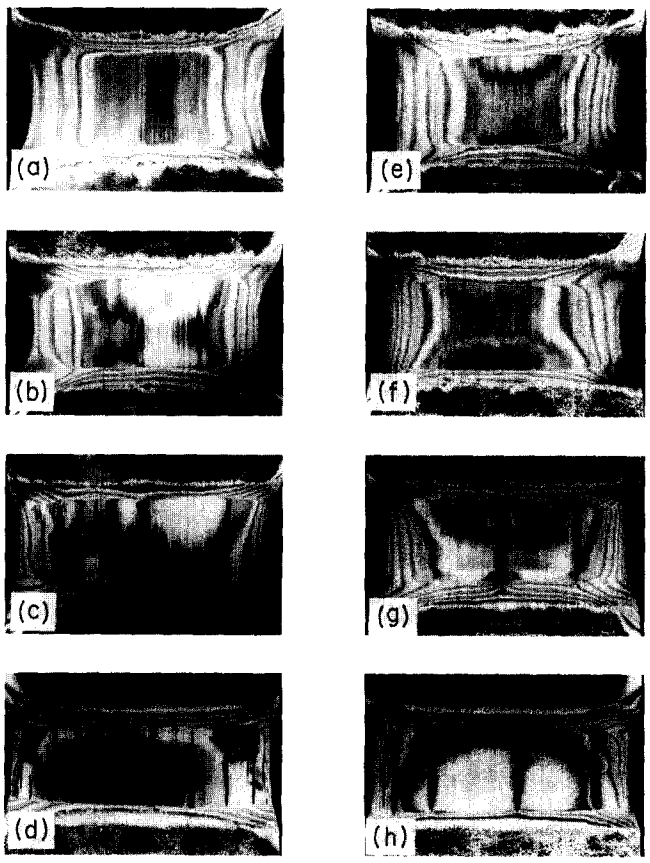

Figure 7 Photographs of films drawn in close-to plane strain conditions at the same macroscopic strain $\Lambda \approx 3$: copolymer A at draw temperatures (*a*) 80°C, (*b*) 120°C, (*c*) 140°C, (*d*) 160°C; copolymer DC at draw temperatures (*e*) 120°C, (*f*) 140°C, (*g*) 160°C, (*h*) 180°C (crossed polarizers; draw axis vertical)

of bulk samples (see *Figure 6b*). Fissures seldom occur in the middle of the samples, some exceptions being due to morphological defects that involve stress concentrations.

In the case of films, the defect width compares with the sample thickness, so that, in contrast to thick plates, through-voids are formed. However, the fact that both kinds of sample, having different surface textures, exhibit the same type of transverse craze-like defect at high temperature shows that this is an intrinsic phenomenon of the mechanism of plastic deformation of EVOH copolymers.

It is to be noticed that the craze-like defects discussed above are only related to the crazes of glassy polymers from a morphological standpoint[20]. They are quite different from true crazes from a phenomenological standpoint. Indeed, 'crazing' is the typically brittle mode of deformation of glassy or semi-crystalline polymers far below the glass transition temperature. True crazes lead to failure through transverse crack propagation, but with increasing temperature they are gradually replaced by the ductile 'shear banding' deformation mode, resulting in the so-called brittle-to-ductile transition. On the contrary, the phenomenon observed in the EVOH copolymers preferentially occurs at high temperature. In addition, the present craze-like defects turn into longitudinal fissures instead of transverse cracks. Finally, the size of the present defects is much larger than that of true crazes. So the origin of the two kinds of deformation defect should be quite different. It is suggested that the fissuring trend of EVOH copolymers is due to a drop in the cohesive energy.

The draw ratio is a factor of considerable importance in the fissuring phenomenon. *Figure 9* shows that a copolymer DC film that is drawn in plane strain conditions at 140°C may display fissures provided that deformation is performed up to the macroscopic strain $\Lambda = 3.5$ (*Figure 9a*), whereas no fissures are observed for $\Lambda = 3$ (*Figure 7f*). Drawing much beyond this strain entails multiplication of fissures initiated from the neck shoulder close to the machine grips (*Figure 9b*). In contrast, when drawn at 160°C, i.e. somewhat below the melting point, copolymer DC exhibits fissures in the early stage of necking. Indeed, a lenticular neck forms at $\Lambda = 1.5$ (*Figure 9c*), then fissures occur at $\Lambda = 1.8$ as the neck begins to expand (*Figure 9d*).

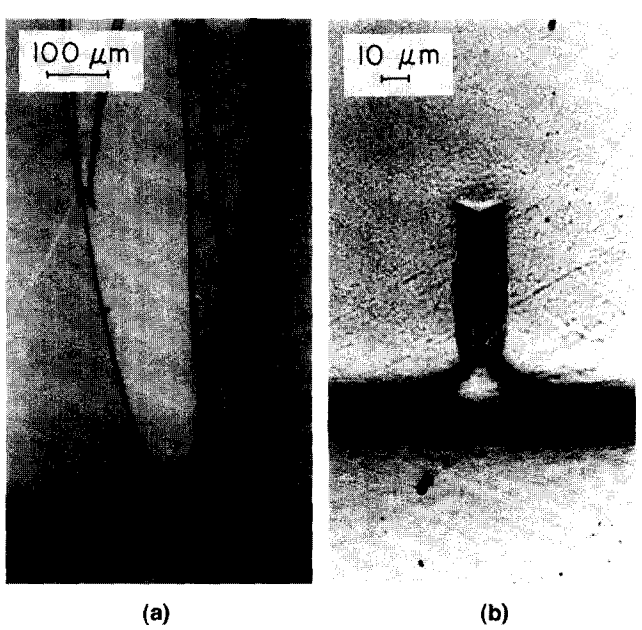

Figure 8 Optical micrographs of (*a*) propagating fissures in a thin film of copolymer A drawn at $T_d = 120$°C and of (*b*) a local defect precursory of a fissure (unpolarized light; draw axis vertical). Reproduced from Ref. [14] with permission of the ASME

Evidence of a structural change in the crystal

The draw-temperature-dependent change of morphological characteristics of the plastic deformation of the copolymers suggests that there is a structural modification in the materials for a critical temperature of about 100°C. This is supported by the yield stress data of the predrawn samples. A preliminary X-ray diffraction study of samples drawn at temperatures of 80 and 150°C shows a clear disorganization of the crystalline phase at low temperature, as reported in *Figure 11*. The two main reflections characteristic of the monoclinic phase of PVOH[21] and vinyl-alcohol-rich EVOH copolymers[22,23] give rise to well separated equatorial spots for the sample drawn at high temperature (*Figure 10a*). In contrast, a single equatorial spot occurs for the sample drawn at 80°C (*Figure 10b*). The latter finding suggests a strain-induced phase change of the monoclinic form into a disordered crystalline form of mesomorphic character. The eventual transformation of the crystalline phase into an amorphous state, as suggested by Yoshida *et al.*[24] is thoroughly ruled out for the

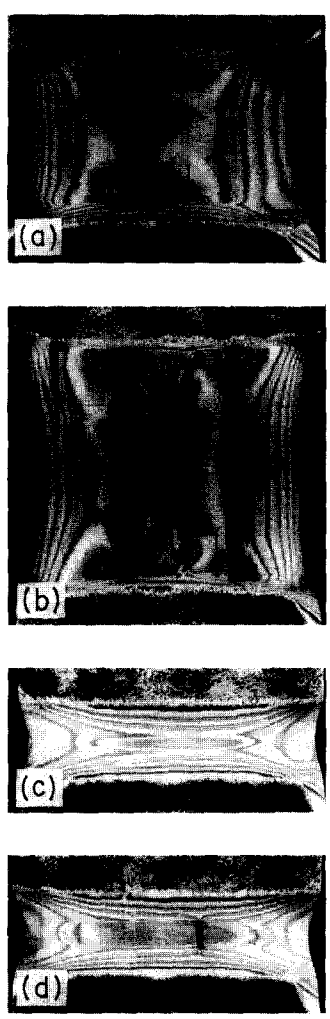

Figure 9 Photographs of films of copolymer DC drawn in plane strain conditions for two macroscopic strains: $T_d = 140$°C, (*a*) $\Lambda = 3.5$, (*b*) $\Lambda = 5$; $T_d = 160$°C, (*c*) $\Lambda = 1.5$, (*d*) $\Lambda = 1.8$ (crossed polarizers; draw axis vertical)

following reasons:

(1) the disorganization occurs above the glass transition temperature;
(2) the unique X-ray reflection is only about 2° wide at half height, i.e. not large enough to be consistent with an amorphous disorder;
(3) a crystal-like order is preserved along the fibre axis.

The two latter points are discussed in an accompanying paper[25]. As a matter of fact, in addition to the broad equatorial diffraction, apart from the zeroth-order strata of the fibre diagram, clear-cut first-order strata having slightly diffuse spots are observed on the long exposure X-ray pattern of copolymer A drawn at 80°C. This pattern is fairly consistent with that of copolymer A fibre drawn at 150°C, as well as with the PVOH fibre diagram[26]. This is evidence that a crystalline order exists along the chain axis upon drawing at low temperature, in spite of the strong disorder created in the basal plane of the crystal unit cell.

The WAXS patterns of copolymer DC drawn at 150 and 80°C are reported in *Figure 11*. They show conspicuously that the vinyl alcohol richer copolymer also undergoes a disorganization of the crystalline phase upon drawing at 80°C. This finding suggests that the strain-induced phase transition is a general trend of EVOH copolymers.

Interpretation of the mechanical behaviour

Porter and coworkers[27-29] have extensively studied the strain-induced phase change that occurs in PP under compressive testing. This phenomenon is very similar to that reported above for the case of EVOH, since a mesomorphic crystalline form is involved in the plastic deformation process of PP below 70°C, this phase being metastable above T_g. Saraf and Porter[30] have further discussed the general phenomenon of phase transformation upon deformation in semi-crystalline polymers. They concluded that a metastable disordered phase is an intermediate state towards plastic deformation thanks to its looser chain packing compared with the stable crystal.

So, in the present case of the EVOH copolymers, a strain-induced disordered phase may be the reason for the improved plastic properties for draw temperatures below 100°C. The sheet-like structure of the stable crystalline form of EVOH copolymers is suspected to be the main prejudicial factor for good plastic properties. The monoclinic structure of PVOH and EVOH copolymers[26,31] is shown in *Figure 12*, together with that of orthorhombic PE for comparison. It is obvious that the sheet-like structure displays a strong mechanical anisotropy because of the v.d.w. interactions between the sheets compared with the strong hydrogen-bonds (H) within the sheets[32]. Increasing the temperature will involve a collapse of the inter-sheet v.d.w. bonds before that of the intra-sheet H-bonds. This decay should occur in a range of temperature close to the melting point of PE, owing to the paraffin-like nature of the v.d.w. bonds. One may even expect a slightly lower temperature than that of the PE melting, since the average distance between the (100) planes of the sheet structure is slightly greater than that of the corresponding planes of the PE crystal cell and the v.d.w. bonds should, consequently, be weaker. In this connection, PVOH displays a clear-cut transition at about 110°C in the rate of variation with temperature of the (100) spacing[17] which is evidence of the decay of the inter-sheet interactions. Such a structure composed of strong sheets with weak interactions is capable of giving rise to the peculiar morphological features of necking at 120°C, notably the fissure-initiating craze-like defects. Indeed, the easy glide of the unique slip system composed of the H-bonded sheets is likely to turn quickly into cracks that can propagate from

Figure 10 WAXS patterns of copolymer A samples drawn at (*a*) T_d = 150°C and (*b*) T_d = 80°C, for a draw ratio $\lambda \approx 6$ (draw axis vertical)

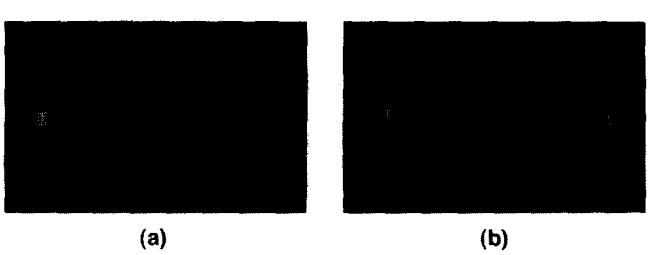

Figure 11 WAXS patterns of copolymer DC samples drawn at (*a*) T_d = 150°C and (*b*) T_d = 80°C, for a draw ratio $\lambda \approx 6$ (draw axis vertical)

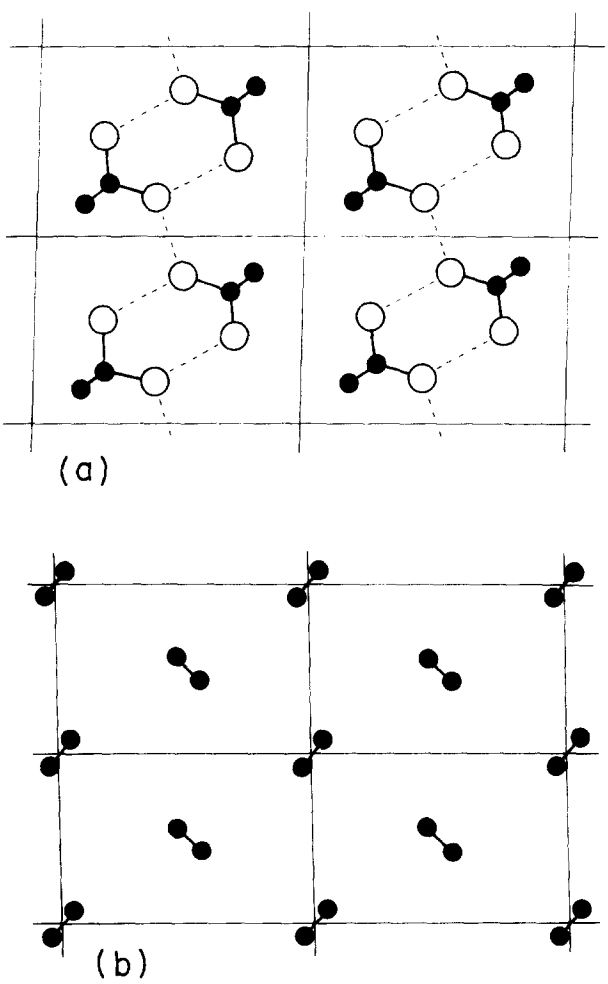

Figure 12 Unit cells of (*a*) monoclinic EVOH and (*b*) orthorhombic PE (view in projection on the basal plane)

any crystal to the neighbouring ones, giving rise to macroscopic fissures. The chain folds that bridge the slip planes are suspected to produce the fibrils within the craze-like defects (*Figures 6b* and *8b*).

In the isotropic materials, the crystals having their sheet structure perpendicular to the draw direction are prone to split into separated sheets since the principal tensile stress is acting normal to their surface. However, the microscopic cracks between the sheets are not able to grow into macroscopic cracks or fissures because the average orientation of the surrounding crystals prevents fissure propagation, as depicted in *Figure 13a*. Dealing with the crystals that are not oriented perpendicular to the draw direction, normal stresses due to local stress triaxiality may also separate the sheets. As soon as a neck occurs, involving a high strain gradient, the crystals quickly rotate towards a common orientation of the sheets close to the draw direction. Then, for temperatures above the collapse of the v.d.w. sheet interactions, the tensile normal stress component works as the driving force for the propagation of the splitting of the sheet structure over macroscopic distances through the roughly aligned crystals, as sketched in *Figure 13b*.

It is worth noticing that fissures do not develop upon uniaxial tensile deformation, but the propensity does exist. Indeed, the drawn samples display longitudinal splitting at room temperature if bent or twisted.

Conversely, the phase change that occurs at low draw temperatures is likely to disturb, and even destroy, the sheet-like structure, leading to a mechanically more isotropic structure. The fact that the two main reflections merge into a single spot is suggestive of a unique plane family with high symmetry about the chain axes. A corollary is a random distribution of the H-bonds about the chain axes.

It was mentioned in the Introduction section that polyamides exhibit similar trends towards drawing as do PVOH and EVOH copolymers. First of all, it is to be noticed that quenched polyamide 6 exhibits a mesomorphic structure[33,34] that is significantly more ductile than the crystalline form of annealed polyamide 6.[35,36] The mesomorphic structure has a hexagonal symmetry which affords a mechanical isotropy about the chain axes. Borrowing from this analogy, the improved orientation capacity of the EVOH at low temperature can be definitively ascribed to the disordered crystalline structure which should be mechanically more isotropic about the chain axis than the monoclinic form owing to the lateral chain disorder.

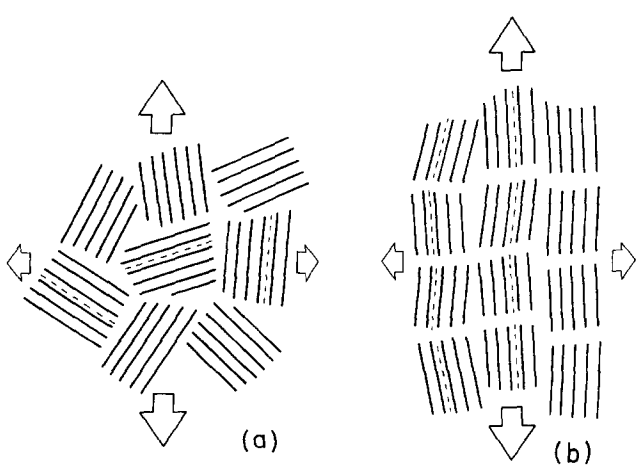

Figure 13 Schematic picture of the sheet-like crystals in plane strain tensile deformation: (*a*) isotropic texture, (*b*) oriented texture (the dotted line represents an inter-sheet crack; draw axis vertical)

The ability for biaxial orientation of EVOH copolymers below 100°C, that has been claimed to result from a reduced orientation-induced crystallization rate[3], is more likely due to the structural change involving a mesomorphic form which is less stiff and more ductile than the stable form that prevails at high temperatures. For the sake of comparison, linear high density PE can be biaxially oriented at temperatures close to the melting point in spite of its high orientation-induced crystallization rate. However, owing to its orthorhombic unit cell, this polymer exhibits mechanical isotropy about the chain axis in the crystal.

A detailed investigation of the disordered phase is reported in the second paper of this series, with a discussion on the way it may occur in relation to temperature and draw ratio, as well as quenching treatment.

CONCLUSION

Strong changes in the mechanical properties of EVOH copolymers have been shown to occur at about 100°C. In the low temperature range, the copolymers deform plastically through diffuse necking. In the high temperature range, sharp necks may take place, depending on the crystallinity and melt index, accompanied by a strong propensity for fissures and cracks. A structural transition from the monoclinic crystalline form to a mesomorphic form below 100°C has been disclosed for draw ratios $\lambda > 4$. This strain-induced metastable crystalline structure is mechanically more isotropic and more ductile than the monoclinic stable structure. It is suggested that the ability for biaxial orientation of the materials at low temperature is governed by the mechanical properties of the new strain-induced structure rather than by the temperature dependence of the orientation-induced crystallization rate.

ACKNOWLEDGEMENTS

The authors are indebted to ELF-ATOCHEM for financial support and permission for publishing this work.

REFERENCES

1. Iwanami, T. and Hirai, Y., *Tappi J.*, 1983, **66**, 85.
2. Combellick, W. A., in *Encyclopedia of Polymer Science and Engineering*, Vol. 2, eds H. M. Mark, N. M. Bikales, C. G. Overberger and G. Menges. John Wiley, New York, 1988, pp. 176–192.
3. Okaya, T. and Ikari, K., in *Polyvinyl Alcohol Developments*, ed. C. A. Finch. John Wiley, New York, 1992, Chapter 8.
4. Adams, G. C., in *Structure and Properties of Polymer Films*, eds R. W. Lenz and R. S. Stein. Plenum Press, New York, 1973, pp. 169–189.
5. de Vries, A. J., *Polym. Eng. Sci.*, 1983, **23**, 241.
6. Karacan, I., Taraiya, A. K., Bower, D. I. and Ward, I. M., *Polymer*, 1993, **34**, 2691.
7. Adams, G. C., *J. Polym. Sci. Polym. Phys. Ed.*, 1971, **9**, 1235.
8. Kyu, T., Fujita, K. and Cho, M. H., *Polym. Eng. Sci.*, 1989, **29**, 383.
9. Gerrits, N. S. J. A., Young, R. J. and Lemstra, P. J., *Polymer*, 1990, **31**, 231.
10. Masuda, M., in *Polyvinyl Alcohol Developments*, ed. C. A. Finch. John Wiley, New York, 1992, Chapter 12.
11. Galeski, A., Argon, A. S. and Cohen, R. E., *Macromolecules*, 1988, **21**, 2761.
12. Galeski, A., Argon, A. S. and Cohen, R. E., *Macromolecules*, 1991, **24**, 3945.
13. Galeski, A., Argon, A. S. and Cohen, R. E., *Macromolecules*, 1991, **24**, 3953.
14. Djezzar, K., Lefebvre, J. M., Séguéla, R. and Germain, Y., *Am. Soc. Mech. Eng. Appl. Mech. Div.*, 1995, **203**, 115.

15. Apicella, A., Hopfenberg, H. B. and Piccarolo, S., *Polym. Eng. Sci.*, 1982, **22**, 382.
16. Garrett, P. D. and Grubb, D. T., *J. Polym. Sci. Polym. Phys. Ed.*, 1987, **25**, 2509.
17. Hong, P. O. and Myasaka, K., *Polymer*, 1991, **32**, 3140.
18. Macknight, W. J. and Tetreault, R. J., *J. Polym. Sci. Polym. Symp.*, 1971, **35**, 117.
19. Starkweather, H. W. Jr, Avakian, P., Fontanella, J. J. and Wintersgill, M. C., *Plast. Rub. Comp. Process. Appl.*, 1991, **16**, 255.
20. Crazing in polymers, *Adv. Polym. Sci.* 1983, **52–53**.
21. Tadokoro, H., *Structure of Crystalline Polymers*. Wiley-Interscience, New York, 1979, pp. 68–69.
22. Matsumoto, T., Nakamae, K., Ogoshi, N., Kawasoe, M. and Oka, H., *Kobunshi Kagaku*, 1971, **28**, 610.
23. Matsumoto, T., Nakamae, K., Oka, H. and Kawarai, S., *Sen-i-Gakkaishi*, 1974, **30**, 391.
24. Yoshida, H., Tomizawa, K. and Kobayashi, Y., *J. Appl. Polym. Sci.*, 1979, **24**, 2277.
25. Penel, L., Djezzar, K., Lefebvre, J. M., Séguéla, R. and Fontaine, H., *Polymer*, in press.
26. Tadokoro, H., *Structure of Crystalline Polymers*. Wiley-Interscience, New York, 1979, pp. 153–154.
27. Saraf, R. F. and Porter, R. S., *Mol. Cryst. Liq. Cryst. Lett.*, 1985, **2**, 85.
28. Saraf, R. F. and Porter, R. S., *Polym. Eng. Sci.*, 1988, **28**, 842.
29. Osawa, S. and Porter, R. S., *Polymer*, 1994, **35**, 545.
30. Saraf, R. F. and Porter, R. S., *J. Polym. Sci. Polym. Phys. Ed.*, 1988, **26**, 1049.
31. Wunderlich, B., *Macromolecular Physics, Vol. 1: Crystal Structure, Morphology, Defects*. Academic Press, 1973, pp. 108–110.
32. Nakamae, N., Kamayema, M. and Matsumoto, T., *Polym. Eng. Sci.*, 1979, **19**, 572.
33. Sandeman, I. and Keller, A., *J. Polym. Sci.*, 1956, **19**, 401.
34. Ziabicki, A., *Kolloid Z. Z. Polym.*, 1959, **167**, 132.
35. Hoashi, K., Kawasaki, N. and Andrews, R. D., in *Structure and Properties of Polymer Films*, ed. R. W. Lenz and R. S. Stein. Plenum Press, New York, 1973, p. 283.
36. Murthy, N. S., *Polym. Commun.*, 1991, **32**, 301.